

SINGLE-TRIAL EXTRACTION OF VISUAL EVOKED POTENTIALS FROM THE BRAIN

Mohd Zuki Yusoff, Nidal Kamel, Ahmad Fadzil Mohd Hani

Electrical & Electronic Engineering Department, University Teknologi PETRONAS
Bandar Seri Iskandar, 31750 Tronoh, Perak, MALAYSIA
phone: + (605) 368 7807, fax: + (605) 365 7443, email: mzuki_yusoff@petronas.com.my
web: http://www.utp.edu.my

ABSTRACT

Estimating a visual evoked potential (VEP) from the human brain is challenging since its signal-to-noise ratio (SNR) is generally very low. An eigendecomposition-based subspace approach originally proposed for enhancing speech corrupted by colored noise, has been investigated and tested in the single trial extraction of VEPs. This scheme arbitrarily labeled as an eigen-decomposition (ED) method has been compared with a third-order correlation (TOC) method, using both realistic simulation and real human data. The results produced by the ED algorithm show much cleaner waveforms, and higher degree of consistency in detecting the P100, P200, and P300 peaks.

Keywords: Eigenvalue decomposition, subspace methods, visual evoked potential latencies.

1. GENERAL INFORMATION

Visual evoked potential (VEP) latencies such as the P100's are used by clinicians to check the integrity of the visual pathways from the retina to the occipital cortex part of the brain [1]. The VEP is not immediately distinguishable from the brain recording because the VEP is buried deep inside the ongoing electroencephalogram (EEG) noise, with a typical signal-to-noise ratio (SNR) of -5 to -10 dB [2]. The EEG is highly colored with unknown covariance matrix.

Conventionally, ensemble averaging is used to extract the VEPs. For this, hundreds of trials need to be acquired and averaged out to really produce clean VEP estimates; this requires very long recording time causing discomfort and fatigue to the subject under study. Among the most recent "single-trial" approaches to detect VEPs is a third-order correlation (TOC) technique proposed by Gharieb and Cichocki [3]. This technique performs well in handling white and colored noise whose spectrum does not overlap with that of the desired signal. However, the efficiency of the TOC method is compromised when spectrum overlapping occurs.

The focus of this study is to correctly estimate VEP latencies, instead of VEP amplitudes. In general, an approach based on a signal subspace principle performs well in estimating the desired peak positions (i.e., latencies) of a given waveform. The VEP extraction method presented here is inspired by work from a speech enhancement area, originally proposed

by Ephraim and Van Trees [4]; the original work dealt primarily with white noise. Later, Rezayee and Gazor [5] extended the time-domain-constrained white noise method to deal with colored noise by approximating the covariance matrix of the Karhunen-Loève transform (KLT) noise vectors with a diagonal matrix.

In this paper, we apply the mathematical model suggested by [4] and introduce the estimator enhanced by [5] to extract the VEP latencies from the colored EEG noise, without using a pre-whitening process. The incorporation of universal optimization schemes in [4] and [5] makes them suitable for our single-trial estimation of VEPs.

2. MODEL DEVELOPMENT

2.1 VEP Model

In developing a mathematical expression for extracting a VEP signal, the following model is defined.

$$\mathbf{y} = \mathbf{x} + \mathbf{n} \quad (1)$$

where, \mathbf{y} is the M-dimensional vector of the corrupted (noisy) VEP signal; \mathbf{x} is the M-dimensional vector of the original (clean) VEP signal; \mathbf{n} is the M-dimensional vector of the additive EEG noise which is assumed to be uncorrelated with \mathbf{x} . Next, \mathbf{H} is defined as the M x M-dimensional matrix of the VEP time-domain constrained linear estimator.

Further, $\hat{\mathbf{x}}$ is defined as the M-dimensional vector of the estimated VEP signal. The estimated VEP signal $\hat{\mathbf{x}}$ is related to \mathbf{H} and \mathbf{y} in the following way:

$$\hat{\mathbf{x}} = \mathbf{H}\mathbf{y} \quad (2)$$

The estimated VEP signal $\hat{\mathbf{x}}$ will never be exactly equal to the original VEP signal \mathbf{x} ; errors will inevitably be produced in the estimated VEP signal. In the case of VEP estimation, the system equation in (2) is to minimize a specified error criterion, which is the ultimate measure of the VEP estimation performance criterion. As such, the error signal $\boldsymbol{\varepsilon}$ obtained by [4] is given by:

$$\begin{aligned} \boldsymbol{\varepsilon} &= \hat{\mathbf{x}} - \mathbf{x} = \mathbf{H}\mathbf{y} - \mathbf{x} = (\mathbf{H} - \mathbf{I})\mathbf{x} + \mathbf{H}\mathbf{n} \\ &= \boldsymbol{\varepsilon}_x + \boldsymbol{\varepsilon}_n \quad \text{where } \boldsymbol{\varepsilon}_x = (\mathbf{H} - \mathbf{I})\mathbf{x}, \quad \boldsymbol{\varepsilon}_n = \mathbf{H}\mathbf{n} \end{aligned} \quad (3)$$

The ε_x represents the VEP distortion and ε_n represents the residual noise. The energies of the signal distortion

$$\begin{aligned}\bar{\varepsilon}_x^2 &= \text{tr}\left(\mathbb{E}\left\{\varepsilon_x \varepsilon_x^T\right\}\right) \\ &= \text{tr}\left((\mathbf{H} - \mathbf{I})\mathbf{R}_x(\mathbf{H} - \mathbf{I})^T\right)\end{aligned}\quad (4)$$

where \mathbf{R}_x is the VEP covariance matrix

and the energies of the residual noise

$$\begin{aligned}\bar{\varepsilon}_n^2 &= \text{tr}\left(\mathbb{E}\left\{\varepsilon_n \varepsilon_n^T\right\}\right) \\ &= \text{tr}\left(\mathbf{H}\mathbf{R}_n\mathbf{H}^T\right)\end{aligned}\quad (5)$$

where \mathbf{R}_n is the EEG noise covariance matrix

lead to the total residual energies

$$\bar{\varepsilon}^2 = \bar{\varepsilon}_x^2 + \bar{\varepsilon}_n^2 \quad (6)$$

The EEG noise covariance matrix \mathbf{R}_n can be obtained from the pre-stimulation EEG samples, during which the VEP signals are absent. Our ultimate goal is to minimize both the unwanted energies so that a minimal error signal is obtained. The challenge is when signal distortion is at its lowest, noise will be at its highest; on the other hand, if noise is fully minimized, distortion will be at its greatest. Therefore, a good balance needs to be exercised so that the noise residues can be reasonably minimized without introducing significant distortion to the processed signal.

2.2 Estimator Optimization

Now, the aim is to design a linear estimator \mathbf{H} that minimizes the VEP signal distortion over all linear filters. This can be achieved by maintaining the residual noise within a permissible level. Mathematically, the optimum linear estimator \mathbf{H}_{opt} with time-domain constraints on the residual noise is formulated by [4] as

$$\mathbf{H}_{opt} = \min_{\mathbf{H}} \bar{\varepsilon}_x^2 \quad \text{subject to: } \bar{\varepsilon}_n^2 \leq M\sigma^2 \quad (7)$$

where M is the dimension of the noisy vector space and σ^2 is a positive constant noise threshold level. The σ^2 in (7) dictates the amount of the residual noise allowed to remain in the linear estimator. Next, the Lagrangian function in association with the ‘‘Kuhn-Tucker necessary conditions for constrained minimization’’ [4] are applied to (7) to obtain \mathbf{H}_{opt} . The formed Lagrangian function can be expressed as

$$\mathbf{L}(\mathbf{H}, \mu) = \bar{\varepsilon}_x^2 + \mu(\bar{\varepsilon}_n^2 - M\sigma^2) \quad (8)$$

where μ is the Lagrange multiplier. It follows that the filter matrix \mathbf{H} is a stationary feasible point if it satisfies the following gradient equation $\nabla_{\mathbf{H}}\mathbf{L}(\mathbf{H}, \mu) = 0$:

$$\begin{aligned}\frac{\partial \mathbf{L}(\mathbf{H}, \mu)}{\partial \mathbf{H}} &= \frac{\partial}{\partial \mathbf{H}} [\bar{\varepsilon}_x^2 + \mu(\bar{\varepsilon}_n^2 - M\sigma^2)] = 0 \\ \Rightarrow \frac{\partial}{\partial \mathbf{H}} [\text{tr}((\mathbf{H} - \mathbf{I})\mathbf{R}_x(\mathbf{H} - \mathbf{I})^T)] &+ \frac{\partial}{\partial \mathbf{H}} [\mu \text{tr}(\mathbf{H}\mathbf{R}_n\mathbf{H}^T)] = 0 \quad (9) \\ \Rightarrow 2(\mathbf{H} - \mathbf{I})\mathbf{R}_x + 2\mu\mathbf{H}\mathbf{R}_n - 0 &= 0\end{aligned}$$

Subsequently, the gradient equation in (9) can be solved as

$$\mathbf{H} = \mathbf{R}_x(\mathbf{R}_x + \mu\mathbf{R}_n)^{-1} \quad (10)$$

The filter matrix \mathbf{H} stated in (10) functions as a fixed filter, which performs well to estimate the VEP at a relatively high SNR. As the SNR degrades, it is desirable if \mathbf{H} can be adjusted accordingly to minimize the noise residues while keeping the signal distortion at an acceptable level. The eigendecomposition of \mathbf{R}_x and \mathbf{R}_n components stated in (10) makes \mathbf{H} adjustable; the noisy VEP space can be decomposed separately into signal and noise only subspace. If the dimension of the \mathbf{R}_x eigenvalues is not lowered, the filter \mathbf{H} functions exactly as that denoted in (10) – keeping signal distortion to its very minimum and noise energy to its maximum. A suitable dimension of the \mathbf{R}_x eigenvalues will eliminate the noise only subspace, enabling the VEP to be estimated from the remaining signal subspace. Of course, the wanted signal may not be completely free from noise since the ‘‘signal’’ subspace is actually a ‘‘signal plus noise’’ subspace. Nevertheless, the wanted signal is now clearly visible as the SNR value gets improved due to the subspace filtering technique.

2.3 Generic Subspace Approach

Now, eigenvalue or singular value decomposition can be performed on \mathbf{R}_x and \mathbf{R}_n . By treating $\mathbf{R}_x = \mathbf{U}\mathbf{\Delta}_x\mathbf{U}^T$, we rewrite (10) as

$$\mathbf{H}_{opt} = \mathbf{U}\mathbf{\Delta}_x(\mathbf{\Delta}_x + \mu\mathbf{U}^T\mathbf{R}_n\mathbf{U})^{-1}\mathbf{U}^T \quad (11)$$

where, \mathbf{H}_{opt} denotes an optimal estimator; \mathbf{U} is the unitary eigenvector matrix produced from a symmetric basis matrix $\mathbf{\Sigma}$ which is to be computed from the proper combinations of \mathbf{R}_x and \mathbf{R}_n terms; $\mathbf{\Delta}_x$ is the diagonal eigenvalue matrix of \mathbf{R}_x .

It should be noted that the Lagrange multiplier μ has to be set to a proper value. The higher value of μ eliminates more noise residues at the expense of higher distortion in the recovered VEP.

Theoretically, the linear estimator in (11) functions optimally if the unitary eigenvector matrix \mathbf{U} derived from $\mathbf{\Sigma}$ is able to simultaneously diagonalize both \mathbf{R}_x and \mathbf{R}_n . The full diagonalization of their eigenvalues can be obtained if and only if \mathbf{R}_x and \mathbf{R}_n multiplication is commutative (i.e., $\mathbf{R}_x\mathbf{R}_n = \mathbf{R}_n\mathbf{R}_x$). In reality, complete diagonalization is not possible since their multiplication is non-commutative.

2.4 Eigenvalue Decomposition (ED) Method

By assuming that the VEP and EEG noise are independent, we get the following

$$\mathbf{R}_y = \mathbf{R}_x + \mathbf{R}_n \quad (12)$$

Next, we assume that $\mathbf{\Sigma} = \mathbf{R}_y$ produces an eigenvector matrix that shall diagonalize both \mathbf{R}_x and \mathbf{R}_n . This choice of $\mathbf{\Sigma}$ is the same as that used by [5]. The eigenvalue matrices of the desired VEP and the unwanted noise are then calculated as follows:

$$\begin{aligned} \mathbf{A}_x &\equiv E[\mathbf{U}^T \mathbf{x} \mathbf{x}^T \mathbf{U}] = \mathbf{U}^T \mathbf{R}_x \mathbf{U} \\ &\approx \mathbf{V}^T \mathbf{R}_x \mathbf{V} \end{aligned} \quad (13)$$

$$\begin{aligned} \mathbf{A}_n &\equiv E[\mathbf{U}^T \mathbf{n} \mathbf{n}^T \mathbf{U}] = \mathbf{U}^T \mathbf{R}_n \mathbf{U} \\ &\approx \mathbf{V}^T \mathbf{R}_n \mathbf{V} \end{aligned} \quad (14)$$

Applying (13) and (14) to (11), we approximate our estimator as

$$\mathbf{H}_{ED} = \mathbf{V} \mathbf{A}_x (\mathbf{A}_x + \mu \mathbf{A}_n)^{-1} \mathbf{V}^T \quad (15)$$

Our estimated VEP is then calculated as

$$\hat{\mathbf{x}}_{ED} = \mathbf{H}_{ED} \cdot \mathbf{y} \quad (16)$$

2.5 Algorithm Implementation

The proposed approach can be formulated in the following six steps. For each VEP trial:

Step 1: Compute the covariance matrix of the noisy signal \mathbf{R}_y , and the noise covariance matrix \mathbf{R}_n .

Step 2: Perform the eigendecomposition of $\mathbf{Z} = \mathbf{R}_y$, extract the resulting eigenvector matrix \mathbf{V} , and compute the signal and EEG noise eigenvalue matrices \mathbf{A}_x and \mathbf{A}_n , respectively.

Step 3: Assuming that λ_k series represented by $\lambda_1 > \lambda_2 > \lambda_3 \dots \lambda_M$ are the diagonal elements of \mathbf{A}_x sequenced in descending order, approximate the dimension, L , of the VEP signal subspace using the following:

$$L = \arg \left\{ \max_{1 \leq k \leq M} \lambda_k > 0 \right\} \quad (17)$$

Step 4: The gain vector of the estimator is computed as follows:

$$q(i) = \frac{\lambda_x(i)}{\lambda_x(i) + \mu \lambda_n(i)} \quad 1 \leq i \leq L \quad (18)$$

It is generally difficult to estimate the exact value for the Lagrange multiplier μ . However, we set it to 2 to compromise between the amount of signal distortion and noise residues present in the estimator. The gain matrix \mathbf{G} is obtained by diagonalizing the gain vector, \mathbf{q} .

$$\mathbf{G} = \begin{bmatrix} \text{diag}\{q\} & 0 \\ 0 & 0 \end{bmatrix} = \begin{bmatrix} Q & 0 \\ 0 & 0 \end{bmatrix} \quad (19)$$

Step 5: The sub-optimal linear estimator \mathbf{H}_{ED} is determined as follows:

$$\mathbf{H}_{ED} = \mathbf{V} \cdot \mathbf{G} \cdot \mathbf{V}^T \quad (20)$$

Step 6: Estimate the enhanced VEP signal by:

$$\hat{\mathbf{x}}_{ED} = \mathbf{H}_{ED} \cdot \mathbf{y} \quad (21)$$

3. PERFORMANCE EVALUATION

The ED and TOC methods were tested and assessed using artificial and real human data.

3.1 Assessment of the Algorithm using Artificial Data

The clean artificial VEP \mathbf{x} was generated by superimposing several Gaussian functions; the amplitudes, variance and mean of these functions were experimentally tweaked to generate precise peak latencies at 100 ms, 200 ms, and 300 ms, mimicking the real P100 (or P1), P200 (or P2), and P300 (or P3), respectively.

The pre-stimulation EEG colored noise \mathbf{n}_{pre} is generated using autoregressive (AR) model [6] given by the following equation.

$$\begin{aligned} v(n) &= 1.5084v(n-1) - 0.1587v(n-2) - \\ &0.3109v(n-3) - 0.0510v(n-4) + u(n) \end{aligned} \quad (22)$$

The artificial post-stimulation EEG noise \mathbf{n} was generated by manipulating the variance of \mathbf{n}_{pre} to introduce a 10 % error in the artificial pre-stimulation EEG. The artificially-corrupted VEP signal \mathbf{y} was then produced by adding together the artificial VEP \mathbf{x} and the post-stimulation EEG \mathbf{n} .

To test the robustness of both algorithms, the ratio of the signal (i.e., artificial VEP) over the colored noise (i.e., EEG) was varied from approximately +0 dB to -10 dB. The corrupted VEP signal with a specific value of SNR was applied to the inputs of the ED and TOC filters to extract the P100, P200 and P300 components. One hundred different runs were performed for each level of SNR. For successful runs, the values of the extracted peaks were precisely recorded from the filter outputs. On the other hand, **zeros** will be assigned to all VEP peaks in cases where any filters failed to produce the intended waveforms. Later, the P100's, P200's and P300's (from the combinations of successful and unsuccessful trials) of the one hundred trials were individually averaged; these averaged values were thereafter compared with the reference values at 100 ms, 200 ms and 300 ms, respectively.

Table 1 below tabulates the success rates for both estimators over SNR = 0 dB to -10 dB.

Table 1 - The success rates of the ED and TOC filters at SNR = 0 dB to -10 dB.

SNR [dB]	VEP Extraction Success Rate [%]	
	ED	TOC
0	96	65
-2	92	60
-4	92	58
-6	86	55
-8	78	47
-10	86	30

From Table 1, it can be stated that the ED and TOC filters produce success rates at an average of 88 % and 52.5 %, respectively, over the whole SNR range. The efficiency of the ED filter drops slightly as the SNR gets lower. On the other hand, the TOC filter deteriorates drastically as the SNR went below -6 dB.

For some graphical illustrations, samples of various waveforms, with successful extraction of components at -4 dB using both the ED and TOC methods, are shown in Figure 1 below.

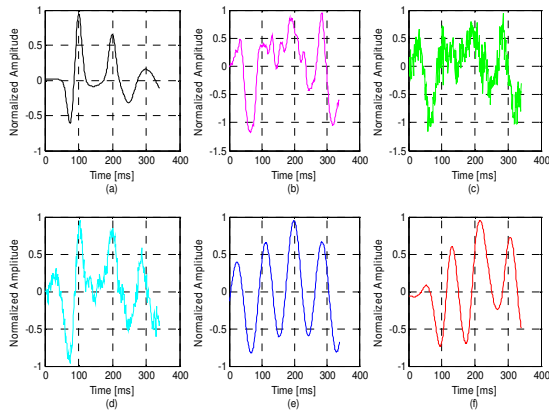


Figure 1 - Samples of various waveforms. (a) The artificial VEP x ; (b) The artificial pre-stimulation EEG noise n_{pre} ; (c) The artificial post-stimulation EEG noise n ; (d) The mixture of the artificial VEP and post-stimulation EEG $y = x + n$, at SNR = -4 dB; The successfully estimated VEP \hat{x}_{ED} , using (e) the ED method, and (f) the TOC approach.

Finally, in order to clearly highlight the filters' performance, another performance metric, measured in terms of percentage errors of VEP peaks versus SNR levels, is tabulated in Table 2 below.

Table 2 - Estimation of the P components using the ED and TOC methods: Percentage errors (PEs) of the averaged P1's (i.e., P100s), P2's (i.e., P200's) and P3's (i.e., P300's) at various SNRs.

SNR [dB]	PE of Averaged P1's [%]		PE of Averaged P2's [%]		PE of Averaged P3's [%]	
	ED	TOC	ED	TOC	ED	TOC
0	10.3	13.2	1.8	20.6	0.6	22.6
-2	9.9	25.6	2.5	31.7	1.0	33.2
-4	6.6	23.2	2.4	32.4	4.5	34.5
-6	7.2	38.5	2.7	45.7	4.8	47.5
-8	0.5	45.8	7.7	52.5	9.1	54.4
-10	11.0	66.7	1.1	71.4	6.3	72.9

From Table 2, it can be deduced that ED introduces a percentage error as high as 11 % (at SNR = -10 dB) for P1

components, 7.7 % (at SNR = -8 dB) for P2 components, and 9.1 % (at SNR = -8 dB) for P3 components.

In addition, the TOC estimator generates 66.7 % percentage error (at SNR = -10 dB) for P1 components, 71.4 % (at SNR = -10 dB) for P2 components, and 72.9 % (at SNR = -10 dB) for P3 components.

3.2 Assessment of the Algorithm using Human Data

Experiments were carried out on **normal** subjects who were asked to watch a checkerboard pattern comprising two different visual stimuli (75% non-target and 25% target) presented in a pseudo-random order (oddball paradigm). For each subject, sixteen different trials were measured and scalp recordings were made according to the International 10/20 System in frontal (F1, F2), central (C3, Cz, C4), parietal (P3, P4) and occipital (O1, O2) electrodes referenced to link earlobes. In this paper, we will show results for **three** artefact-free trials of a subject taken from the left occipital (i.e., O1) electrode only. Each trial containing 512 data points (256 pre- and 256 post-stimulation) was pre-filtered in the range 0.1 to 70 Hz, and was sampled at 250 Hz. More detailed information pertaining to the experimental setup can be found from [7, 8].

Since the experiments dealt only with sixteen trials per subject, the estimated VEP latencies by means of averaging were not readily available; the ensemble averaging technique would normally require a significant number of samples (e.g., 100 or 200) to be taken. Therefore, to make analysis possible, we assume that the subject under study managed to produce valid P1, P2 and P3 components exactly at 100 ms, 200 ms and 300 ms. This imposes the most stringent conditions on the filter performance, yet it provides the most straightforward and consistent basis for our discussions.

Table 3 below summarizes the measured values of P components produced by the ED and TOC filters for the subject's three trials pattern VEP test.

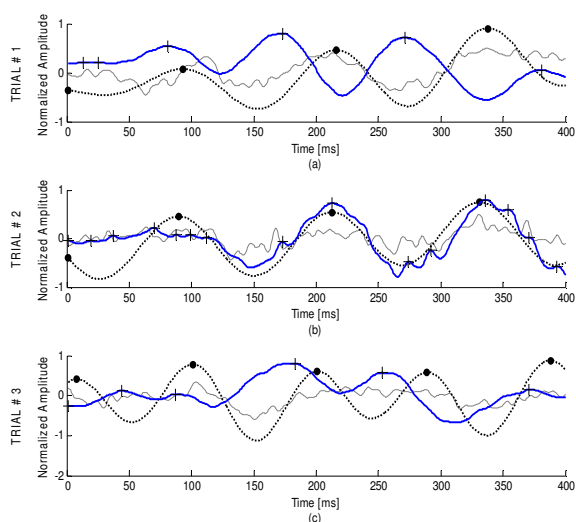
Table 3 - Measured P1, P2 and P3 latencies (in ms) of the subject's three trials Pattern VEP test. The values in the parentheses are the corresponding percentage errors (PEs) when the recorded P1, P2 and P3 values are compared with the reference values at 100 ms, 200 ms and 300 ms, respectively.

Note: NA (i.e., not available) is used whenever a peak of interest is missing or corrupted with noise.

TRIAL #	ED			TOC		
	P1 [ms]	P2 [ms]	P3 [ms]	P1 [ms]	P2 [ms]	P3 [ms]
	(PE [%])	(PE [%])	(PE [%])	(PE [%])	(PE [%])	(PE [%])
1	93 (7)	216 (8)	338 (13)	81 (19)	173 (14)	271 (9.7)
2	90 (10)	213 (6.5)	331 (10)	NA (100)	213 (6.5)	NA (100)
3	101 (1)	201 (0.5)	289 (3.7)	87 (13)	183 (8.5)	253 (16)

If the allowable maximum percentage error (PE) for each P component is set to 15 % (in Table 3 the peaks with PEs of 15 % or less are boldfaced), the ED filter successfully extracted all the required peaks in trials #1, #2 and #3, whereas the TOC estimator managed to extract only the P2 and P3 from trial #1, P2 from trial #2, and P1 and P2 from trial #3.

We present here an illustration of the ED's and TOC's extracted Pattern VEPs in Figure 2.



Note: The point (●) marker is used to denote the peaks extracted by the ED filter. The plus sign (+) marker denotes the peaks extracted by the TOC filter.

Figure 2 - Noisy Pattern VEPs (solid thin gray line) for (a) trial #1; (b) trial #2; (c) trial #3; and their corresponding estimates produced by the ED filter (dotted thick black line) and the TOC estimator (solid thick black line).

From Figure 2, it can be stated that the ED filter produces very clean signals, whereas majority of the TOC filter's estimates still contain noise ripples. In trial #2 for example, the TOC filter produced peaks at 19, 37, 70, 88, 99, 112, 171, 213, 274, 292, 336, 354, 371, and 393 ms. The P2 occurs clearly at 213 ms, but the P1 and P3 cannot be determined absolutely due to the presence of several peaks in the vicinity.

In brief, the simulated and real data experiments proved the superiority of the subspace technique over the third order correlation method.

4. CONCLUSIONS AND FUTURE WORK

A subspace technique for enhancing VEP signals degraded by EEG noise is proposed and thoroughly tested. Two main experiments involving realistic simulation and real Pattern VEP data have been conducted on the ED and TOC filters. The results reflect the capability of the subspace technique to become an optimum scheme for extracting VEP embedded inside strong colored noise at an SNR value as low as -10 dB.

Next, comprehensive tests involving larger patient data will be performed. Some modifications will also be made to the ED algorithm to make it more robust. Among the most critical criteria in implementing the ED algorithm is the suitable selection of a basis matrix, leading to the creation of a truly unitary common diagonalizing matrix and resulting in fully optimum VEP extraction.

Presently, the technique is able to satisfactorily estimate the VEP latencies of the P100, P200 and P300. In the future, some mechanisms need to be devised to enable the algorithm to capture both amplitudes and latencies in correlation with the original waveform.

ACKNOWLEDGMENT

We would like to thank Dr. Martin Schürmann of the University of Nottingham, United Kingdom who acquired the Pattern Visual Evoked Potentials data at the Institute of Physiology, Medical University of Lübeck, Germany, and allowed its distribution. We also thank Dr. R. Quian Quiroga of the University of Leicester, United Kingdom for making it available on his webpage.

REFERENCES

- [1] L. Huszar, "Clinical Utility of Evoked Potential," eMedicine, April 18, 2006, retrieved May 5, 2006 from <http://www.emedicine.com/neuro/topic69.htm>.
- [2] G. Henning and P. Husar, "Statistical Detection of Visually Evoked Potentials," IEEE Engineering in Medicine and Biology, July/August 1995.
- [3] R. R. Gharieb and A. Cichocki, "Noise Reduction in Brain Evoked Potentials Based on Third-Order Correlations," IEEE Transactions on Biomedical Engineering, vol. 48, no. 5, pp. 501-512, May 2001.
- [4] Y. Ephraim and H. L. Van Trees, "A Signal Subspace Approach for Speech Enhancement," IEEE Transaction on Speech and Audio Processing, vol. 3, no. 4, pp. 251-266, July 1995.
- [5] A. Rezayee and S. Gazor, "An Adaptive KLT Approach for Speech Enhancement," IEEE Transactions on Speech and Audio Processing, vol. 9, no. 2, February 2001.
- [6] X. H. Yu, Z. Y. He and Y. S. Zhang, "Time-Varying Adaptive Filters for Evoked Potential Estimation," IEEE Transactions on Biomedical Engineering, vol. 41, no. 11, November 1994.
- [7] R. Quian Quiroga and M. Schürmann, "Functions and Sources of Event-Related EEG Alpha Oscillations Studied with Wavelet Transform," Elsevier Clinical Neurophysiology, 110 (1999), pp. 643-654.
- [8] R. Quian Quiroga and H. Garcia, "Single-Trial Event-Related Potentials with Wavelet Denoising," Elsevier Clinical Neurophysiology, 114 (2003), pp. 376-390.